



This is a repository copy of *Exchange between drainage systems and surface flows during urban flooding: Quasi-steady and dynamic modelling in unsteady flow conditions*.

White Rose Research Online URL for this paper:
<https://eprints.whiterose.ac.uk/176672/>

Version: Published Version

Article:

Kitsikoudis, V., Erpicum, S., Rubinato, M. et al. (4 more authors) (2021) Exchange between drainage systems and surface flows during urban flooding: Quasi-steady and dynamic modelling in unsteady flow conditions. *Journal of Hydrology*, 602. 126628. ISSN 0022-1694

<https://doi.org/10.1016/j.jhydrol.2021.126628>

Reuse

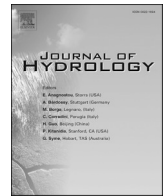
This article is distributed under the terms of the Creative Commons Attribution (CC BY) licence. This licence allows you to distribute, remix, tweak, and build upon the work, even commercially, as long as you credit the authors for the original work. More information and the full terms of the licence here:
<https://creativecommons.org/licenses/>

Takedown

If you consider content in White Rose Research Online to be in breach of UK law, please notify us by emailing eprints@whiterose.ac.uk including the URL of the record and the reason for the withdrawal request.



eprints@whiterose.ac.uk
<https://eprints.whiterose.ac.uk/>



Exchange between drainage systems and surface flows during urban flooding: Quasi-steady and dynamic modelling in unsteady flow conditions

Vasileios Kitsikoudis^{a,*}, Sebastien Erpicum^b, Matteo Rubinato^{a,c,d}, James D. Shucksmith^e, Pierre Archambeau^b, Michel Pirotton^b, Benjamin Dewals^b

^a Water Engineering and Management, Faculty of Engineering Technology, University of Twente, Enschede, the Netherlands

^b Hydraulics in Environmental and Civil Engineering, Urban and Environmental Engineering, University of Liege, 4000 Liege, Belgium

^c Faculty of Engineering, Environment and Computing, School of Energy, Construction and Environment, Coventry University, Coventry CV1 5FB, UK

^d Centre for Agroecology, Water and Resilience, Coventry University, Wolston Lane, Coventry CV8 3LG, UK

^e Department of Civil and Structural Engineering, Mappin Building, S1 3JD, University of Sheffield, Sheffield, UK

ARTICLE INFO

This manuscript was handled by Corrado Corradini Editor-in-Chief, with the assistance of Valentina Ciriello, Associate Editor

Keywords:

Sewer/surface flow interactions
Urban flood modelling
Drainage systems
Head losses
Unsteady flow
Urban hydraulics

ABSTRACT

The accurate modelling of urban flooding constitutes an integral part of flood risk assessment and management in residential and industrial areas. Interactions between drainage networks and surface runoff flows are commonly modelled based on weir/orifice equations; however, this approach has not been satisfactorily validated in unsteady flow conditions due to uncertainties in estimating the discharge coefficients and associated head losses. This study utilises experimental data of flow exchange between the sewer flow and the floodplain through a manhole without a lid to develop two alternate approaches that simulate this interaction and describe the associated exchange flow. A quasi-steady model links the exchange flow to the total head in the sewer pipe and the head losses in the sewer and the manhole, whilst a dynamic model takes also into account the evolution of the water level within the manhole at discrete time steps. The developed numerical models are subsequently validated against large-scale experimental data for unsteady sewer flow conditions, featuring variable exchange to the surface. Results confirmed that both models can accurately replicate experimental conditions, with improved performance when compared to existing methodologies based only on weir or orifice equations.

1. Introduction

Urban flooding events tend to become more frequent due to the increase of urbanization and changes in rainfall patterns linked with climate change. An accurate quantification of flood risk is important for assessing relative vulnerability under given and predicted rainfall events in order to develop cost effective asset investments and flood mitigation approaches. In urban areas, hydrodynamics associated with flood events is particularly complex because such events commonly include interactions between surface flows/runoff and flows within urban drainage networks (Schmitt et al., 2004; Rubinato et al., 2019). The risk of flooding is commonly evaluated using hydraulic modelling tools, which utilize a number of empirical and semi-empirical relationships (and associated parameters) to simulate processes such as runoff and frictional/turbulent energy losses, including relationships to describe interactions between surface flows and drainage networks (Djordjević et al., 2005; Leandro et al., 2009; Seyoum et al., 2012). However, despite

recent advances in remote sensing and open access data (Moy de Vitry et al., 2017; Moy de Vitry and Leitão, 2020), there is a general paucity of high-resolution datasets for flood model validation (Tscheikner-Gratl et al., 2016). Typical datasets consisting of point depth of flow observations during flood events are insufficient to fully overcome parameter non-identifiability/equifinality issues in complex flood models, or provide a detailed evaluation of modelling representations for individual model components such as above/below ground flow exchange (Beven, 2006; Dottori et al., 2013; Arrault et al., 2016).

Datasets collected during detailed, controlled laboratory studies can be used to validate hydraulic models (Martins et al., 2017; Martins et al., 2018) and/or provide an improved understanding of physical processes and flood model parameters such as energy loss coefficients (Hare, 1983). However, transferring findings from scaled laboratory studies into practice can be challenging. For example, due to its significance in urban flood modelling, a number of experimental studies have investigated common representations of flow exchange between surface flows

* Corresponding author.

E-mail address: v.kitsikoudis@utwente.nl (V. Kitsikoudis).

<https://doi.org/10.1016/j.jhydrol.2021.126628>

Received 13 March 2021; Received in revised form 20 June 2021; Accepted 25 June 2021

Available online 10 July 2021

0022-1694/© 2021 The Author(s). Published by Elsevier B.V. This is an open access article under the CC BY license (<http://creativecommons.org/licenses/by/4.0/>).

and urban drainage networks through hydraulic structures such as manholes and gullies. Flow exchange through such structures can be bi-directional (net exchange to the surface or the drainage network), and hydraulic conditions associated with these situations are generally unsteady and highly three dimensional (Lopes et al., 2015; Beg et al., 2018). Within network scale urban flood models such interactions are commonly represented by simple weir/orifice equations with net flows given as a function of hydraulic/pressure head difference between surface flow and the drainage network, the geometrical properties of the structure and an energy loss term (Nasello and Tucciarelli, 2005; Chen et al., 2007; Seyoum et al., 2012). To evaluate this approach some studies have calibrated/validated urban drainage/flood models based on physical models of urban catchments with multiple exchange structures (Bazin et al., 2014; Fraga et al., 2015; Noh et al., 2016; Dong et al., 2021), whilst other work has directly measured flow rates through individual interaction structures, allowing a direct comparison between exchange equations and measurements. For example, Rubinato et al. (2017) conducted a detailed experimental study of the weir and orifice equations representation of exchange flows through a scaled open manhole in both drainage and surcharging conditions. In steady flow conditions with subcritical surface flows, discharge coefficients were calibrated based on flow, pressure and depth measurements in the pipe network and on the surface and found to be constant over the range of tested flow conditions. However, calculated coefficients were sensitive to flow depth/pressure values used within the calibration, which may in practice be calculated with different methods and vary over the longitudinal profile of the hydraulic structure. In addition, when calibrated relationships were used to validate a numerical model against a range of unsteady flow events, meaningful differences were observed between predicted and observed exchange volumes.

Several other laboratory studies have been conducted to calibrate weir/orifice equations for a range of grate types and steady flow conditions. Martins et al. (2014) focused on drainage flows into a gully pot, while Gómez et al. (2019) and Rubinato et al. (2018a) investigated drainage flows through different grate types and Kemper and Schlenkhoff (2019) analyzed supercritical flows over road drainage grates. All these studies have provided a wide range of recommended discharge coefficients, likely due to the sensitivity of energy loss processes to the geometry of different structures, but also potentially due to methodological differences in the definition of surface and drainage system hydraulic head (e.g. measurement location), how geometrical properties are defined (e.g. calculation of grate void spaces or the wetted perimeter) and how partially/fully submerged grate/manhole openings are considered. Hence the accurate representation of flood inundation processes in urban areas may require site specific calibration of discharge coefficients (Dong et al., 2021), which is unfeasible in most practical applications.

Based on the studies described above, a number of issues concerning the suitability of weir/orifice type methodologies to describe above/below ground flow interaction can be identified as follows: 1. Outstanding uncertainty regarding the discharge coefficient, which past work has shown to differ significantly from common standard values for classical weirs/orifices and thus requires site specific calibration or experimental/numerical studies for accurate identification (Martins et al., 2014; Gómez et al., 2019). 2. Lack of understanding of the hydraulically effective area of a drainage inlet during shallow flows and how this changes with flow depth and/or velocity (Martins et al., 2018). 3. The sensitivity of the calculated exchange discharge (and/or discharge coefficient) to the measurement of hydraulic head (Bazin et al., 2014; Rubinato et al., 2018b), which can vary significantly within and across hydraulic structures (Marsalek, 1985). 4. A lack of successful validation of the approach in unsteady flow exchange conditions through individual structures (Rubinato et al., 2017).

Flows which surcharge from or enter into drainage systems may also be considered as diverging or converging junction flows respectively, both of which have been extensively studied on a fundamental level

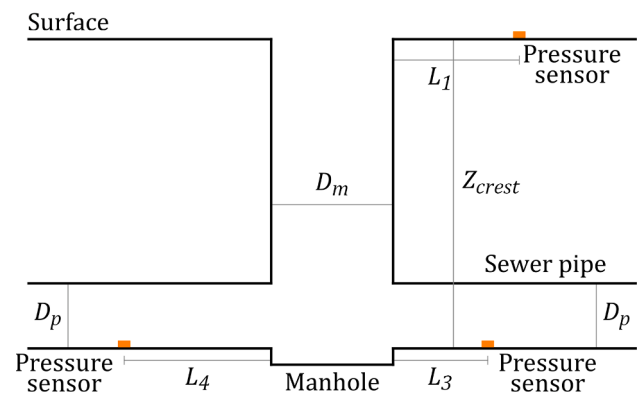


Fig. 1. Schematic diagram of the experimental setup of Rubinato et al. (2017) (figure not to scale).

(McNown, 1954; Graber, 2010), although commonly in pipe diameters much smaller than those found in drainage networks. Bazin et al. (2014) separated the path of surcharging or drainage pipe flow into successive sections, corresponding each to a specific head loss: linear head loss in the pipe, head loss at a division or a junction, or head loss between the surface and the sewer grate. It is also possible to conceptualize an interaction node such as a manhole as a storage element with levels that rise and fall depending on net inflows and outflows through a time varying event. Hence, by utilizing more universal concepts associated with energy losses in diverging and converging flows, more generally applicable methodologies may be determined.

This paper develops and presents two analytical modelling approaches to represent exchange flows between piped drainage and surface flows via exchange structures such as manholes and gullies. A number of experimental datasets described in Rubinato et al. (2017) are used to calibrate the models in steady flow conditions and validate the models using a series of unsteady flow events. The models performance is compared to both experimental data as well the widely used weir/orifice based approaches that represent the current state of the art.

2. Data from large-scale laboratory experiments

The experiments were conducted within a facility constructed from PVC in the water laboratory of the Civil and Structural Engineering Department at the University of Sheffield (Rubinato, 2015). This experimental facility consists of a sewer pipe system with no slope that is linked via a manhole to a hypothetical urban floodplain characterized by a slope of 0.001. Fig. 1 provides a schematic diagram of the experimental setup. The sewer system was constructed based on a 1/6 geometrical scale of a typical UK urban drainage system, while the urban floodplain is 4 m wide and 8 m long and it is 0.478 m above the invert level of the pipe. This height is denoted as Z_{crest} . The internal diameter of the manhole, D_m , is equal to 240 mm, while the internal diameter of the sewer pipe, D_p , is equal to 75 mm both upstream and downstream of the manhole. In the following, the cross-section of the manhole and of the sewer pipe are denoted as A_m and A_p , respectively. Flow discharges were measured with electromagnetic flowmeters in the floodplain upstream, Q_1 , and downstream, Q_2 , of the manhole, and in the sewer pipes also upstream, Q_3 , and downstream, Q_4 , of the manhole. Q_e denotes the exchange flow between the top of the manhole and the surface flow. In the laboratory experiments, Q_e was not measured directly but, for steady-state flow conditions, it can be estimated from the difference between Q_3 and Q_4 which were both measured. Pressure sensors provided the pressure head in the floodplain upstream of the manhole, h_{p1} , and in the sewer pipes upstream, h_{p3} , and downstream, h_{p4} , of the manhole. The pressure heads in pipes with unsteady flow were smoothed in this study by using the median value of five to eight seconds, depending on the case. The horizontal distances of the pressure sensors from the

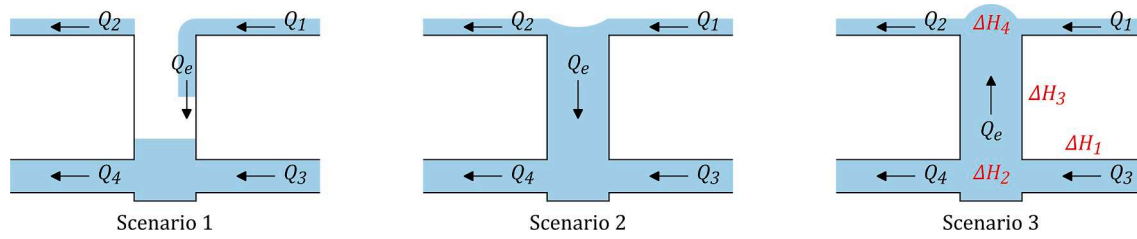


Fig. 2. The three flow scenarios observed during a hydrograph (adapted from Rubinato et al., 2017). In Scenario 3, $\Delta H_1 - \Delta H_4$ denote the head losses that occur at different segments.

nearest edge of the manhole were $L_1 = 340$ mm for the pressure sensor in the floodplain and $L_3 = 230$ mm and $L_4 = 400$ mm for the pressure sensors in the sewer pipes upstream and downstream of the manhole, respectively (Fig. 1). More details about the experimental facility, the instrumentation and the test program are provided in Rubinato (2015) and Rubinato et al. (2017).

Rubinato et al. (2017) analyzed both steady and unsteady flow cases and their extensive dataset is reanalyzed in the present study. This dataset is the only currently openly available dataset on unsteady flow through an individual drainage/exchange structure. The only additional data that are analyzed herein and were not presented in Rubinato et al. (2017) are the pressure head data, h_{p4} , in the downstream sewer pipe (Rubinato, 2015). From the steady state tests, 15 cases with the non-surcharging sewer (Scenario 1 in Fig. 2) and eight cases with the surcharging sewer (Scenario 3 in Fig. 2) condition are considered here. For the nine unsteady flow tests, the flow on the floodplain was maintained constant at 8.15 l/s while a flood hydrograph was run through the sewer pipe, replicating surface to sewer and sewer to surface flow exchange conditions during each unsteady test. During the experiments, discharge and pressure measurements were recorded every $dt = 0.05$ s. For steady flow experiments, the flow depth at the surface was measured at the location of the pressure sensor (Fig. 1), while for the unsteady flow experiments, the flow depth was estimated from the equation of Manning, with a Manning roughness coefficient equal to 0.009 (from prior calibration), similar to an approach adopted in Rubinato et al. (2017).

3. Methods

The modelling methodologies analysed here aim at computing the exchange discharge, Q_e , between a manhole and the surface during an unsteady event in a dual drainage system. The exchange discharge Q_e is defined positive when the exchange flow goes towards the floodplain (surcharging sewer). The two models that are presented in this section are referred to as “quasi-steady model” and “dynamic model”, respectively.

In our quasi-steady model, we follow a similar approach as Rubinato et al. (2017), which regards the pipe-manhole system as a flow junction ($Q_e \leq 0$) or bifurcation ($Q_e > 0$). Nonetheless, compared to the weir/orifice flow exchange approach evaluated in Rubinato et al. (2017), we claim that our quasi-steady model introduces more physics in the calculation of Q_e . Firstly, we link the exchange flow discharge to the total head in the upstream pipe, while Rubinato et al. (2017) considered only the pressure head. Secondly, for the case of surcharging flow from the manhole to the floodplain, we account explicitly for four different contributions to the overall head losses between the pipe and the surface, similar to Bazin et al. (2014) for flow exchange between a street and an underground drainage pipe. Subsequently, we utilise the Bernoulli equation to describe the flow exchange, whereas the approach tested in Rubinato et al. (2017) lumped the influence of all head losses into a single calibrated orifice equation discharge coefficient. This is detailed in Section 3.5. In our new dynamic model, we additionally take into account the evolution with time of the water level, h_m , in the manhole during an unsteady flow event. This evolution cannot be

expressed in quasi-steady models and it provides a better representation of transient effects in the computation of the exchange discharge Q_e because the storage capacity in the manhole is accounted for explicitly. Calibration of the models was performed in steady flow conditions, due to the ability to directly measure the flow rate and hence identify the energy loss parameters, without the need for more complex model calibration methodologies (e.g. Noh et al., 2016). Model validation (or evaluation) is commonly undertaken after model calibration as a method of determining the ability of the model to replicate observed parameters without further modifications from the user (McMillan et al., 2016). To quantify any resulting uncertainties when simulating dynamic events, in this study validation was performed in unsteady flow conditions. The models are presented analytically in the following subsections.

3.1. Flow scenarios

The model evaluated in Rubinato et al. (2017) as well as the two models presented here share the same typology of flow scenarios; but some refinements are introduced here. For this purpose, we define notation H_m to refer to the flow head at the interaction node (manhole), which may be approximated using different methods for the different models. The reference datum is the sewer pipe invert (Fig. 1). Three different flow scenarios may occur (Fig. 2), depending on the value of the head H_m in the manhole with respect to the elevation of the floodplain, Z_{crest} , and the head of the flow in the floodplain, H_s , which is equal to $(Q_1/(W h_s))^2/(2g) + Z_{crest} + h_s$, where W and h_s are the width of and the flow depth in the floodplain, respectively.

- Scenario 1: free weir flow from the floodplain to the manhole ($Q_e < 0$), if the head in the manhole is lower than the level of the floodplain ($H_m \leq Z_{crest}$);
- Scenario 2: submerged weir or orifice flow from the floodplain to the manhole ($Q_e < 0$), if the head in the manhole is higher than the level of the floodplain but lower than the head of the surface flow ($Z_{crest} < H_m \leq H_s$);
- Scenario 3: overflow from surcharging sewer to the floodplain ($Q_e > 0$), if the head in the manhole is greater than the head of the surface flow ($H_m > H_s$).

3.2. Approximation of head within the manhole/pipe network based on the different models

The models presented herein and the models evaluated in Rubinato et al. (2017) differ in the level of detail in which they define and estimate for different flow conditions the total head of the flow in the manhole, and hence the head of the sewer network flow at the point it interacts with the surface flow:

- Rubinato et al. (2017) calibrated the orifice flow exchange equation based on the pressure head h_{p3} at the location of the pressure sensor in the upstream pipe.
- In the quasi-steady model, we approximate H_m by $H_3 - \Delta H_{tot}$, with $H_3 = (Q_3/A_p)^2/(2g) + h_{p3}$ the total head at the pressure sensor in the

upstream pipe and ΔH_{tot} the total head losses between the location of this pressure sensor and the point of flow interaction (Fig. 2) (see details in Section 3.5.1). For non-surcharging conditions, head losses due to Q_e do not occur, as there is no upward flow in the manhole, and the total head losses ΔH_{tot} are noted as ΔH_0 .

- In the dynamic model, H_m is simply taken equal to the water depth, h_m , in the manhole assuming the velocity head in the manhole is negligible. Note that the variable h_m is not considered in the other two models.

3.3. Mass balance in the manhole

Like in a pipe junction or bifurcation, the mass balance in the quasi-steady model can be written as:

$$Q_4 = Q_3 - Q_e \quad (1)$$

where the upstream discharge Q_3 in the pipe is a prescribed boundary condition and the exchange discharge Q_e is predicted by the model. Therefore, the discharge Q_4 in the downstream pipe can be determined directly from Eq. (1).

Unlike the quasi-steady model, the dynamic model considers the manhole as a tank in which the volume of water varies in time with the contributing discharges, according to:

$$A_m \frac{dh_m}{dt} = Q_3 - Q_e - Q_4 \quad (2)$$

Like in the quasi-steady model, the upstream pipe discharge Q_3 is a prescribed boundary condition and the exchange discharge Q_e is estimated by the model. However, Eq. (2) is now necessary to update the value of h_m for the subsequent time step. Therefore, in the dynamic model, the discharge Q_4 in the downstream pipe needs to be computed separately. This step is further described in Section 3.5.2. In steady flow conditions, the mass balance in Eq. (2) reduces to Eq. (1) as in the quasi-steady model.

3.4. Non-surcharging sewer (surface to sewer exchange)

For non-surcharging flow conditions ($Q_e \leq 0$), the quasi-steady and the dynamic model have similar exchange equations with the model tested in Rubinato et al. (2017), with the only difference being the utilization of the total head in the surface flow instead of just using the flow depth:

- in Scenario 1 ($H_m \leq Z_{crest}$), a weir equation is used to describe free flow from the floodplain to the manhole:

$$Q_e = -\frac{2}{3} C_1 \pi D_m \sqrt{2g(H_s - Z_{crest})^3} \quad (3)$$

with C_1 a discharge coefficient to be calibrated;

- in Scenario 2 ($Z_{crest} < H_m \leq H_s$), a submerged weir equation is used when $H_s - Z_{crest} \leq A_m / (\pi D_m)$:

$$Q_e = -C_2 \pi D_m (H_s - Z_{crest}) \sqrt{2g(H_s - H_m)} \quad (4)$$

where C_2 is also a discharge coefficient whose value needs to be determined. When $H_s - Z_{crest} > A_m / (\pi D_m)$, a submerged orifice equation may be used (Rubinato et al., 2017); however, this threshold is not exceeded in our study.

Rubinato et al. (2017) used experimental observations in steady conditions to calibrate parameters C_1 and C_2 . Here, we recalibrated the value of C_1 with the same data as Rubinato et al. (2017) for Scenario 1 (see the expected values in Fig. 6 in Rubinato et al. 2017), but with the surface flow head instead of the flow depth (Eq. 3). The calibration performed by Rubinato et al. (2017) for parameter C_2 involved less data points and led to discontinuities in the computed exchange flow

Table 1

Parameterization of the head of the flow in the manhole, H_m , and calibration parameters for the examined models.

H_m	Rubinato et al. (2017) h_{p3}	Quasi-steady model $H_3 - \Delta H_{tot}$	Dynamic model h_m
C_1	0.54	0.38	0.38
C_2	0.056	$2/3 \times 0.38$	$2/3 \times 0.38$
C_3	0.167	–	0.168

discharge at the transition between Scenarios 1 and 2 (see Figure 10 in Rubinato et al., 2017). Therefore, in the models introduced here, we simply set $C_2 = 2/3 C_1$, which ensures continuity between the exchange discharges computed by Eqs. (3) and (4) when $H_m = Z_{crest}$. Compared to the strategy followed by Rubinato et al. (2017), the continuity between Scenarios 1 and 2 is ensured here at the expense of an accurate agreement with calibration data for Scenario 2; but the number of available experimental data for Scenario 2 is limited and this scenario occurs in practice only for a very short period of time during unsteady flow events at the onset and at the end of surcharging flow (rising and falling limbs of the hydrograph). Therefore, the impact of this choice on the overall accuracy of the computed exchange volume over a surcharging flow event is expected to be very small. All calibration parameters are summarized in Table 1.

3.5. Surcharging sewer

3.5.1. Quasi-steady model

In the quasi-steady model, the overflow discharge from the surcharging manhole to the floodplain is computed from a Bernoulli equation written between the upstream sewer pipe (at the pressure sensor location) and the surface flow, and by taking into account the total head losses, ΔH_{tot} , along the flow path. Head losses occur at four different locations, as shown in Fig. 2 in Scenario 3, hence $\Delta H_{tot} = \Delta H_1 + \Delta H_2 + \Delta H_3 + \Delta H_4$. Linear head losses ΔH_1 are noted along the sewer pipe due to friction and head losses ΔH_2 occur due to flow division and expansion of the cross-section at the junction where the sewer pipe meets the manhole. Additional energy is dissipated as the water flows upward through the manhole with frictional linear head losses ΔH_3 , and finally head losses ΔH_4 occur as the water exits the manhole to the street. Head losses between the sewer pipe and the surface flow can therefore be described by (Idelchik, 2007; Bazin et al., 2014):

$$H_3 - H_s = \underbrace{\frac{f_{p3} L_3}{D_p} \frac{Q_3^2}{2gA_p^2}}_{\Delta H_1} + \underbrace{k_2 \frac{Q_3^2}{2gA_p^2}}_{\Delta H_2} + \underbrace{\frac{f_m (Z_{crest} - D_p)}{D_m} \frac{Q_e^2}{2gA_m^2}}_{\Delta H_3} + \underbrace{k_4 \alpha_4^2 \frac{Q_e^2}{2gA_m^2}}_{\Delta H_4} \quad (5)$$

where f is a friction coefficient denoted as f_{p3} and f_m for the upstream sewer pipe and the manhole, respectively. The friction coefficient, f , is estimated with the formula of Barr (Machiels et al., 2011) as a function of the roughness height k_s , which is considered equal to 0.0005 mm both for the sewer pipe and the manhole, based on a previous calibration performed by Beg et al. (2020). In Eq. (5), the parameter α_4 is the ratio of flow velocity exiting the manhole to the flow velocity inside the manhole, with α_4^2 being equal to 0.95 (Idelchik, 2007), while the coefficient k_4 is associated with local head losses at the exit of the manhole and is considered equal to 1 (Idelchik, 2007). Hence, the only remaining parameter to be determined in Eq. (5) is the coefficient k_2 associated with head losses due to expansion of the flow from the sewer pipe to the manhole. This parameter is likely to require calibration because the available values in the literature either correspond to ratios A_m / A_p of less than one, e.g. in Idelchik (2007), or to pipes of equal cross-sectional area, e.g. in Hager (2010), while in this case the A_m / A_p ratio is greater than ten. As a result, the available values may not be applicable

3.5.1.1. Calibration procedure.

By rearranging Eq. (5) with the standard

values of parameters k_4 and α_4 , the numerical value of k_2 can be computed as:

$$k_2 = \frac{2gA_p^2}{Q_3^2} \left[H_3 - H_s - \frac{f_{p3}L_3}{D_p} \frac{Q_3^2}{2gA_p^2} - \frac{f_m(Z_{crest} - D_p)}{D_m} \frac{Q_e^2}{2gA_m^2} - k_4\alpha_4^2 \frac{Q_e^2}{2gA_m^2} \right] \quad (6)$$

where all quantities in the right-hand-side of Eq. (6) can be evaluated from experimental steady flow observations of Q_3 , Q_1 , h_s , h_{p3} and Q_e . Note that the total head H_s in the floodplain is measured upstream and not downstream of the manhole. As a result, potential head changes of the surface flow due to the interaction of floodplain flow with the surcharging jet are ignored; however, these head changes are negligible because the floodplain is very wide, and hence the overall difference in surface flow depth and velocity upstream and downstream of the manhole is negligible (Rubinato et al., 2018b).

When plotting the values of k_2 from Eq. (6) as a function of the portion of the pipe inflow discharge being exchanged with the surface, Q_e / Q_3 , it appears that the parameter k_2 varies almost linearly with Q_e / Q_3 (Section 4.1.1). Therefore, we consider the following linear function to parameterize k_2 :

$$k_2 = \alpha \frac{Q_e}{Q_3} + \beta \quad (7)$$

where parameters α and β need to be calibrated with experimental data, as shown in Section 4.1.1.

3.5.1.2. Applying the quasi-steady model. To classify the different flow scenarios (e.g. the transition point between non surcharging and surcharging flows), ΔH_0 (see Section 3.2) is first needed. In Scenarios 1 and 2 there is no upward flow in the manhole and hence no head losses due to Q_e . By substituting $Q_e = 0$ in Eqs. (5) and (7), it follows that the head loss ΔH_0 , introduced in Section 3.2, may be evaluated by:

$$\Delta H_0 = \left(\beta + \frac{f_{p3}L_3}{D_p} \right) \frac{Q_3^2}{2gA_p^2} \quad (8)$$

To classify Scenarios 2 and 3 (transition to surcharging flows) H_m is compared to H_s , with H_m taken equal to $H_3 - \Delta H_0$. In this form, if H_m is lower than H_s , then there is no surcharge and no upward flow in the manhole, while if H_m is greater than H_s , then upward, surcharging flow occurs. In the latter case, the total head in the manhole H_m should then be approximated by $H_3 - \Delta H_{tot}$, which is smaller than $H_3 - \Delta H_0$, because of the inclusion of additional positive parameters in the head losses (Eq. (5)).

After the calibration of the parameter k_2 , the exchange discharge, Q_e , in surcharging flow conditions (Scenario 3) can be estimated with Eq. (5) through an iterative process by testing values of Q_e until the two sides of the equation converge. The needed input parameters are the flow discharge and pressure in the upstream sewer pipe, the flow discharge at the floodplain, and the geometric characteristics of the drainage system and the floodplain.

3.5.2. Dynamic model

Similarly to Rubinato et al. (2017), the dynamic model for surcharging sewer uses simply an orifice equation to estimate the surcharging discharge. Nevertheless, in this case the head in the equation is taken here equal to the water depth in the manhole, h_m .

$$Q_e = C_3 A_m \sqrt{2g(h_m - H_s)} \quad (9)$$

In this case, to determine Q_e , the discharge Q_4 is first needed to compute the water depth in the manhole with Eq. (2). Subsequently, the computed water depth can be used for the estimation of the exchange discharge with Eq. (9). In the dynamic model, the discharge Q_4 is estimated by applying the Bernoulli equation between the top of the surcharging manhole jet and the position of the pressure sensor in the

downstream sewer pipe (Fig. 1) where a head, H_4 , boundary condition is set. Local head losses between the manhole jet and H_4 are expressed similarly to the quasi-steady model. To simplify the computations, the head losses in the manhole, i.e., ΔH_3 and ΔH_4 in Eq. (5), are omitted because they are considered negligible as shown by the results of the quasi-steady model (Section 4.1.1). Hence, the Bernoulli equation between the water surface in the manhole and a point in the downstream sewer pipe that is located at a distance L_4 from the downstream edge of the manhole takes into account local contraction losses as the flow exits the manhole, as well as frictional losses in the pipe. Assuming the losses from the contraction form a similar relationship with the flow partition as in Eq. (7), the Bernoulli equation with the aid of Eq. (1) can be written as:

$$h_m - H_4 = \left(\alpha' \frac{Q_3 - Q_4}{Q_4} + \beta' + f_{p4} \frac{L_4}{D_p} \right) \frac{Q_4^2}{2gA_p^2} \quad (10)$$

where f_{p4} is the friction coefficient for flow in the downstream sewer pipe.

3.5.2.1. Calibration procedure. Based on observed data of steady surcharging flow, parameters α' and β' in Eq. (10) may be determined by a linear regression with $(Q_3 - Q_4)/Q_4$ being the independent variable. However, this requires the prior knowledge of h_m . This is attained by applying the Bernoulli equation between the location of the pressure transducer in the sewer pipe upstream of the manhole and the top of the surcharging manhole jet, as follows:

$$H_3 - h_m = f_{p3} \frac{L_3}{D_p} \frac{Q_3^2}{2gA_p^2} + k_2'' \frac{Q_3^2}{2gA_p^2} \quad (11)$$

This equation has a similar structure to Eq. (5) but the head losses in the manhole and in the overflow are considered negligible, similar to Eq. (10), while the coefficient k_2'' differs from k_2 of Eq. (5) because of the utilization of h_m .

The combination of Eqs. (9) and (11), along with the division of both sides of the resulting equation with the velocity head in the upstream sewer pipe and the relationship $Q_3 - Q_4 = Q_e$ in steady surcharging flow conditions, lead to the following non-dimensional equation:

$$(H_3 - H_s) \frac{2gA_p^2}{Q_3^2} - f_{p3} \frac{L_3}{D_p} = \frac{A_p^2}{A_m^2 C_3^2} \left(\frac{Q_3 - Q_4}{Q_3} \right)^2 + k_2'' \quad (12)$$

Based on observed data of steady surcharging flow, the discharge coefficient C_3 can now be estimated with polynomial regression analysis of Eq. (12), with $(Q_3 - Q_4)/Q_3$ being the independent variable. The water depth h_m in the manhole for steady flow conditions can be subsequently calculated with Eq. (9) or Eq. (11) and, finally, the parameters α' and β' in Eq. (10) can be estimated by linear regression.

3.5.2.2. Applying the dynamic model. Given knowledge of the discharge coefficient C_3 and the parameters α' and β' , the exchange discharge, Q_e , and the discharge in the downstream sewer pipe, Q_4 , for surcharging conditions can be estimated for each time step with Eqs. (9) and (10), respectively. The water depth in the manhole is updated at each time step in unsteady flow conditions with Eq. (2). The data requirements of the dynamic model are the flow discharge and pressure in the upstream sewer pipe, the pressure in the downstream sewer pipe, the flow discharge at the floodplain, and the geometric characteristics of the drainage system and the floodplain.

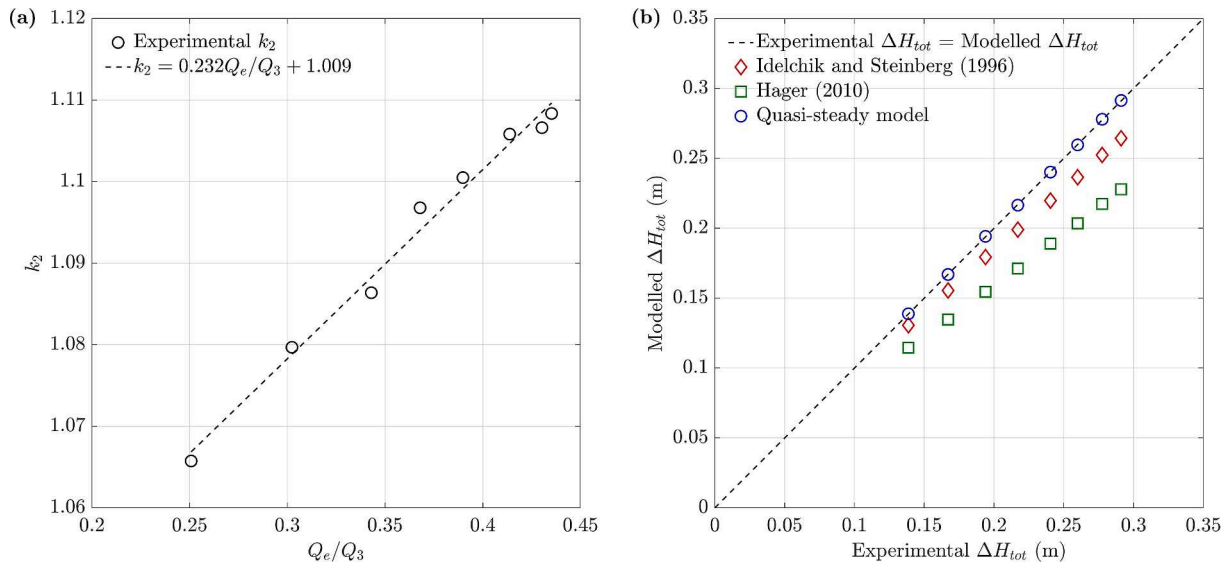


Fig. 3. (a) Linear regression between parameter k_2 and Q_e / Q_3 for the quasi-steady model based on the experimental data of Rubinato et al. (2017) for steady surcharging flow and (b) Comparison of observed (left-hand-side of Eq.(5)) and computed (right-hand-side of Eq.(5)) total head losses from the sewer pipe to the surface for steady surcharging flow.

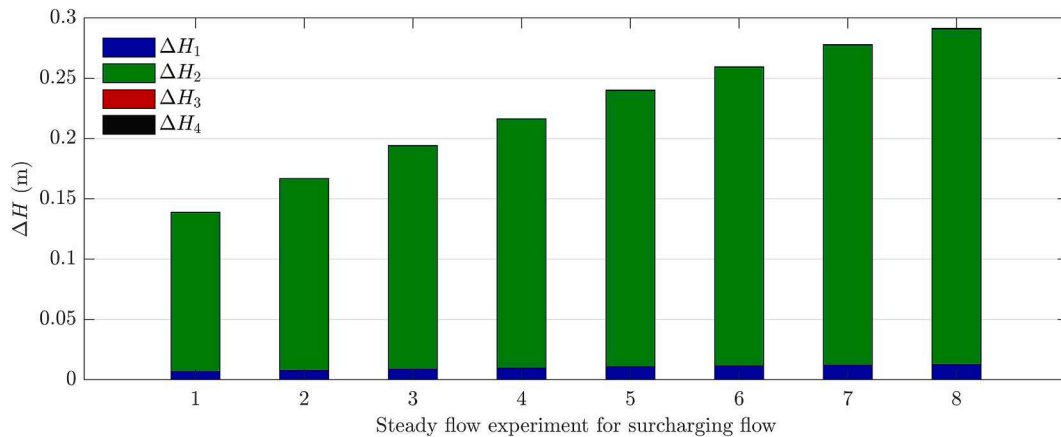


Fig. 4. Distributions of head losses for surcharging sewer under steady flow conditions based on experimental data of Rubinato et al. (2017).

4. Results and discussion

4.1. Calibration of models with steady flow data for surcharging flow conditions

4.1.1. Quasi-steady model

For each of the eight steady-state surcharging flow tests conducted by Rubinato et al. (2017), the numerical value of k_2 was computed from the experimental observations using Eq. (6). When the values of k_2 are plotted against the observed ratios Q_e / Q_3 , the data points follow a linear trend, as demonstrated in Fig. 3a. This confirms the relevance of the parametrization proposed in Eq. (7). By applying linear regression, the coefficients in Eq. (7) are evaluated as $\alpha = 0.232$ and $\beta = 1.009$ (Fig. 3a). Subsequently, the computed total head losses from the sewer pipe to the surface, as modelled based on the right-hand-side of Eq. (5) and with the aid of Eq. (7), are compared to the observed head difference $H_3 - H_s$. As shown in Fig. 3b, the computed values agree well with the measurements.

For the sake of comparison, the total head losses were also computed by estimating the parameter k_2 with the formulae of Idelchik (2007) and Hager (2010), as described in the Appendix. Both of these models underestimate the total head losses (Fig. 3b). The calibrated quasi-steady

model performs slightly better than the formula of Idelchik (2007) and significantly better than the formula of Hager (2010). Although less accurate than the model calibrated here, the formula of Idelchik (2007) still provides a useful value of k_2 to estimate the total head loss in the absence of calibration data.

Fig. 4 shows the head losses that occur at each segment of the system for Scenario 3 (Fig. 2). The total head losses, ΔH_{tot} , depend mostly on the head losses in the second section of the system, ΔH_2 , where the sewer pipe meets the manhole. Specifically, for the eight steady flow experiments of Rubinato et al. (2017) with surcharging flow, ΔH_2 constitutes more than 95% of the total head losses, whereas ΔH_1 is less than 5%, and ΔH_3 and ΔH_4 are approximately 0.01% and 0.1%, respectively. Due to the small contribution of ΔH_4 to the total head loss, the latter is not particularly sensitive to parameters k_4 and α_4 , which justifies the use of standard values.

4.1.2. Dynamic model

Based on the measurements of Rubinato et al. (2017) for steady surcharging flow, the observed values of the left-hand-side of Eq. (12) can be plotted as a function of the measured values of $(Q_3 - Q_4) / Q_3$, as shown in Fig. 5a. A linear regression with $[(Q_3 - Q_4) / Q_3]^2$ being the independent variable, leads to $A_p^2 / (C_3 A_m)^2 = 0.340$, from which it can

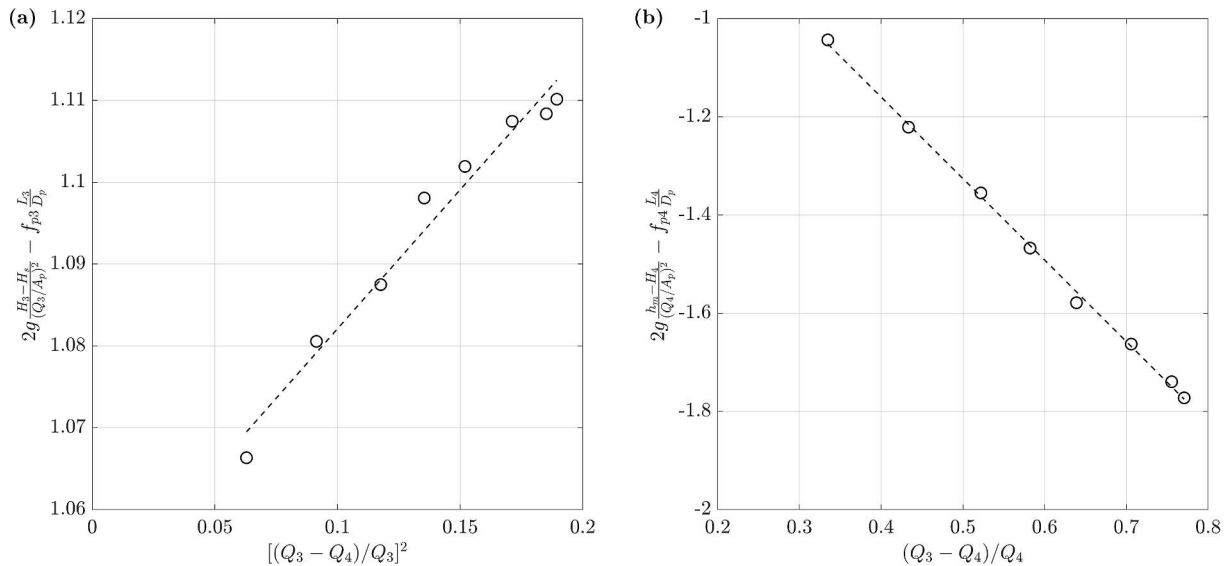


Fig. 5. Calibration of the dynamic model with (a) Linear regression between $[(Q_3 - Q_4)/Q_3]^2$ and the dimensionless head loss from Eq. (12) for the determination of the discharge coefficient C_3 and (b) Linear regression between $(Q_3 - Q_4)/Q_4$ and the dimensionless head loss from Eq. (10) for the determination of parameters α' and β' .

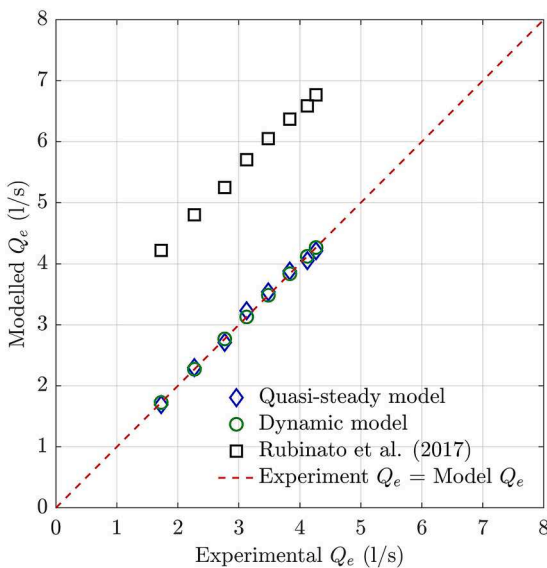


Fig. 6. Comparison of experimental and modelled exchange discharge, Q_e , for surcharging sewer under steady flow conditions. The model tested in Rubinato et al. (2017) was used with its calibrated expected discharge coefficient, with respect to its experimental measurement uncertainty. The data are from the experiments of Rubinato et al. (2017).

be deduced that the discharge coefficient C_3 for the dynamic model is equal to 0.168. The discharge coefficient that was generated with this method is remarkably similar to that estimated by Rubinato et al. (2017) (Table 1), despite the fact that the two methods have notable differences. It should be noted that in Eq. (12), k_2'' was considered to be independent of $(Q_3 - Q_4)/Q_3$, because otherwise a linear dependency would lead to an unrealistic value of C_3 . Subsequently, h_m is calculated from Eq. (9), which allows the application of linear regression in Eq. (10) for the determination of parameters α' and β' . Fig. 5b shows that the linear regression fits the data well with $\alpha' = -1.660$ and $\beta' = -0.496$. Alternatively, in the case of Eq. (11) being used for the calculation of h_m , the parameters α' and β' differ by less than 1%.

The resulting modelled exchange discharges, Q_e , by the quasi-steady

and the dynamic models agree well with the experimental data of Rubinato et al. (2017), as shown in Fig. 6. The results are also compared to the results obtained with the orifice equation calibrated experimentally by Rubinato et al. (2017). The perfect agreement of the dynamic model is owed to the fact that h_m was calculated with Eq. (9) during the calibration process; however, for the validation with unsteady flow conditions h_m will be calculated with Eq. (2). Rubinato et al. (2017) estimated expected values and upper and lower values of the exchange discharge, based on an error parameter associated with the instrumentation error. Our models are compared to the expected values of Rubinato et al. (2017), which overestimate the exchange discharge by approximately 2.5 l/s (Fig. 6). This bias corresponds to the intercept visible in Fig. 8 in Rubinato et al. (2017), which is indeed of the order of 2.5 l/s.

4.2. Validation of models with unsteady flow data

Fig. 7 presents a comparison of the results of the new quasi-steady and dynamic models to the experimental observations and the computations presented in Rubinato et al. (2017), for the nine unsteady experiments reported by Rubinato et al. (2017). The numerical results of Rubinato et al. (2017) displayed in this figure were obtained by using the values of the discharge coefficients C_1 , C_2 , and C_3 calibrated with steady flow experiments ("expected values" in Table 3 of Rubinato et al., 2017) and the observed values of h_{p3} , while h_s was calculated with the equation of Manning. The evolution of the depth h_m in the manhole is computed only by the dynamic model (left column in Fig. 7). In all cases, the dynamic model exhibits a better agreement with the measured data compared to the quasi-steady model and to the model tested in Rubinato et al. (2017) (Table 2), both at the rising and the falling limbs of the hydrographs (right column in Fig. 7). The quasi-steady model performs generally better than the model tested in Rubinato et al. (2017), which overestimates the exchange discharge. This is consistent with the overestimation of the exchange discharge by the model tested in Rubinato et al. (2017) when there is surcharge under steady flow conditions, as highlighted in Fig. 6.

The flow in the drainage system is mostly classified as Scenarios 1 and 3 (Fig. 2), with Scenario 2 occurring only for brief transitional periods of time (Fig. 7 and Table 2). While the transition between Scenarios 1 and 2 is smooth, the transition between Scenarios 2 and 3 can be abrupt, as shown by the dynamic model in Fig. 7. Although the raw

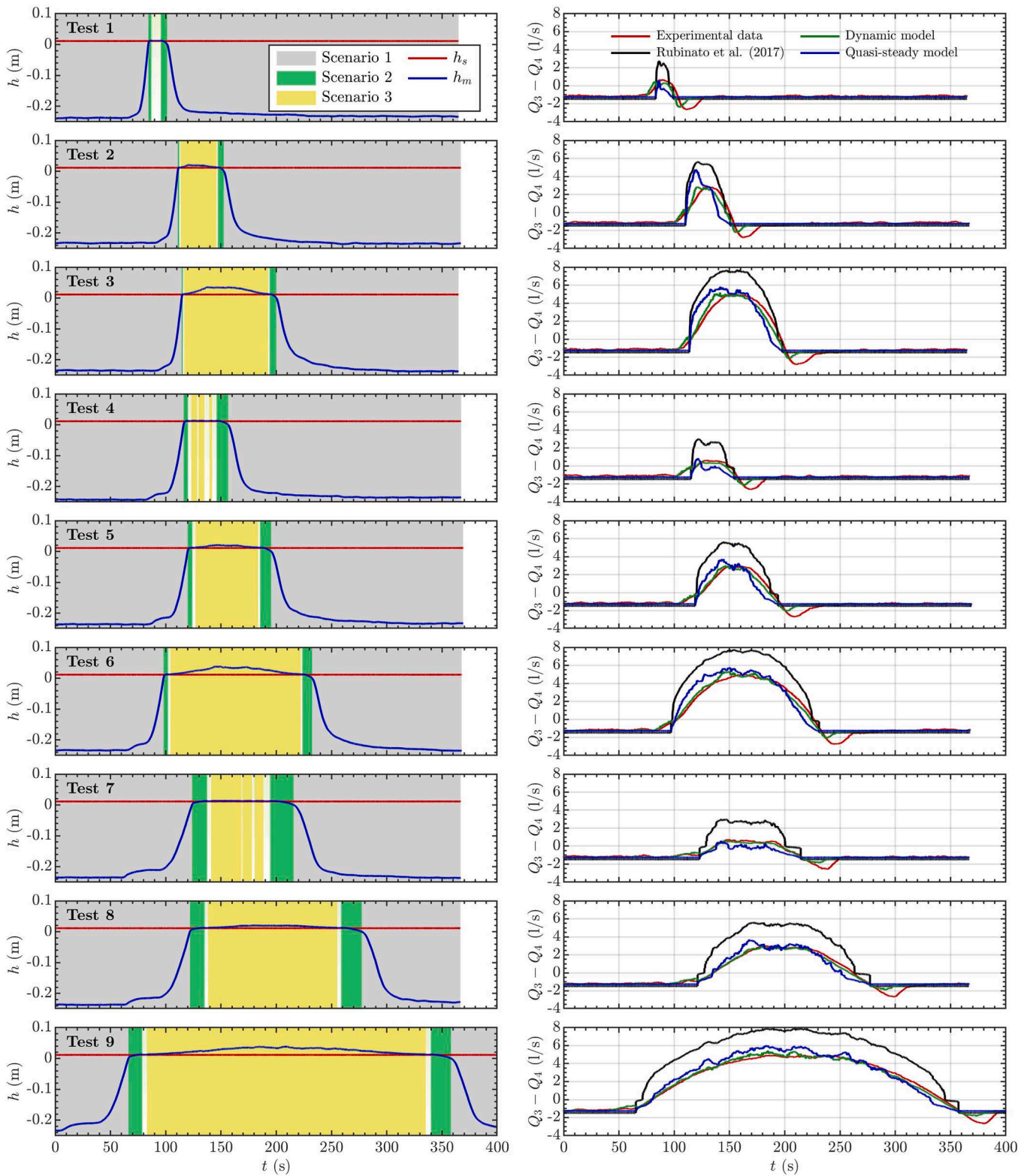


Fig. 7. Evolution of water level in the manhole (left column) and comparison of modelling results for the discharge in the manhole, $Q_3 - Q_4$, (right column) with data from unsteady flow experiments from Rubinato et al. (2017). For the quasi-steady model and the model tested in Rubinato et al. (2017), Q_e was used as a proxy for $Q_3 - Q_4$. In the left column, h denotes the water level with respect to the surface, which is located at $h = 0$, and h_m was computed with the dynamic model. The different scenarios in the left column were determined with the dynamic model with the white areas in between Scenarios 2 and 3 denoting rapid transitions between these scenarios.

Table 2

Percentages of the duration of occurrence of $Q_3 - Q_4 > 0$ for the experimental data and of the occurrence of the three different scenarios for the quasi-steady model, the dynamic model, and the model tested in Rubinato et al. (2017) for the whole duration of each unsteady test. NSE denotes the Nash–Sutcliffe efficiency coefficient for the modelled and measured discharge in the manhole, $Q_3 - Q_4$, for the unsteady part of each hydrograph from Fig. 7. For the quasi-steady model and the model tested in Rubinato et al. (2017), Q_e was used as a proxy for $Q_3 - Q_4$. The model tested in Rubinato et al. (2017) was used with its expected discharge coefficients, with respect to their calibration experimental uncertainty, while the surface flow depth was estimated with the equation of Manning.

		Test 1	Test 2	Test 3	Test 4	Test 5	Test 6	Test 7	Test 8	Test 9
Data: $Q_3 - Q_4 > 0$		4.3%	11.0%	22.6%	7.9%	17.4%	33.6%	16.4%	34.5%	57.4%
Quasi-steady model	Scenario 1	96.1%	89.4%	77.3%	89.8%	80.1%	64.1%	75.5%	57.9%	36.8%
	Scenario 2	3.4%	2.8%	2.8%	8.5%	4.3%	4.6%	18.8%	10.2%	8.2%
	Scenario 3	0.5%	7.8%	19.9%	1.7%	15.2%	31.6%	5.7%	31.8%	55.0%
	NSE	0.338	0.390	0.774	0.427	0.757	0.856	0.634	0.878	0.916
Dynamic model	Scenario 1	95.3%	88.6%	76.5%	89.0%	79.5%	63.4%	74.9%	57.6%	36.4%
	Scenario 2	3.5%	2.2%	2.3%	5.7%	4.5%	4.0%	11.3%	9.6%	7.6%
	Scenario 3	1.2%	9.2%	21.2%	5.3%	16.0%	32.6%	13.8%	32.8%	55.9%
	NSE	0.667	0.874	0.948	0.842	0.938	0.966	0.907	0.967	0.982
Rubinato et al. (2017)	Scenario 1	95.7%	89.0%	77.0%	89.4%	79.7%	63.6%	75.0%	57.5%	36.4%
	Scenario 2	1.2%	1.3%	1.2%	2.1%	2.2%	2.1%	5.5%	5.5%	4.0%
	Scenario 3	3.2%	9.7%	21.8%	8.5%	18.0%	34.3%	19.5%	37.0%	59.6%
	NSE	0.144	0.059	0.412	-0.604	0.093	0.221	-1.265	-0.268	-0.037

pressure input data/measurements in the sewer pipes were filtered to smoothen the time-series, the dynamic model is still sensitive to the unsteadiness of the flow, which leads to rapid fluctuations between Scenarios 3 and 2, (i.e., manhole surcharge or drainage). This sensitivity is particularly evident in tests 1, 4, and 7, where the peaks of the hydrographs are the lowest and the quasi-steady and dynamic models, particularly the former, are not always able to classify correctly when the flow enters Scenario 3, (in which $Q_3 - Q_4 > 0$, Table 2).

For the computations performed with the quasi-steady model and by Rubinato et al. (2017), the calculated exchange discharge Q_e is considered equal to the value of $Q_3 - Q_4$, according to Eq. (1). In contrast, in reality, the exchange discharge Q_e differs from the value of $Q_3 - Q_4$ during transient phases, as a result of variations in the storage in the manhole as expressed by Eq. (2). Here, the experimental dataset reports only $Q_3 - Q_4$ due to the infeasibility of measuring continuously the evolution of Q_e in the laboratory setup (Rubinato, 2015). Only the dynamic model gives access to both Q_e and $Q_3 - Q_4$, as these quantities are computed separately by this model. Fig. 8 shows a comparison between these two discharges obtained from the dynamic model, from which significant overlap can be observed for the largest part of the hydrograph, aside from at the start and the end of the unsteady sections. At the end of the unsteady section of the hydrograph, the suction that is observed in the manhole as the water depth decreases in the transition from Scenario 2 (submerged weir) to Scenario 1 (free weir) is only partially captured by the $Q_3 - Q_4$ results. This is due to the transient nature of the dynamic model and its ability to represent the evolution of storage in the manhole. The abrupt changes between Scenarios 2 and 3 are also evident in the hydrographs of Q_e , where the exchange discharge fluctuates between positive and negative values before it stabilizes. These abrupt transitions in the exchange discharge correspond to the white areas between Scenarios 2 and 3 in Fig. 7 (left column). Despite this sensitivity in the computation of the exchange discharge, the dynamic model results of $Q_3 - Q_4$ agree well with the experimental data.

A quantitative evaluation of the unsteady modelling results for the discharge in the manhole is provided in Table 2, which shows the Nash–Sutcliffe efficiency (NSE) coefficient between the results of each model and the corresponding measurements for the unsteady part of each hydrograph. The NSE coefficient is consistently higher for the dynamic model followed by the quasi-steady model. The performance of both models improves as the surcharge becomes more intense, while the difference between the two models is the lowest for tests 3, 5, 6, 8, and 9, which are cases with high hydrograph peaks and longest duration of the unsteady section (Fig. 7). The modelled and measured net water volumes that are exchanged between the sewer and the floodplain are compared in Fig. 9. A very good agreement is obtained for the dynamic model. In some cases (e.g. Tests 1 and 2), the quasi-steady model seems

to predict the exchanged volume as well as the dynamic model, despite the fact that the overall evolution of the exchange discharge is less accurate than the dynamic model (Fig. 7). In reality, the dynamic model is more reliable since it captures better the governing physics. Nonetheless, considering that the quasi-steady model exhibits a good agreement with the experiments in cases where the flow unsteady hydrograph is long and the suction effect becomes small, it can be inferred that this model remains also valuable, especially given the fact that it does not require a downstream boundary condition when compared to the dynamic model.

5. Concluding remarks

In light of climate change and with the anticipation of an increase in the frequency of extreme rainfall events, the accurate design of drainage systems and accurate evaluation of flood risk is of paramount importance for the resilience of urban areas.

This study developed a quasi-steady and a dynamic model for the determination of the exchange discharge between a sewer pipe and the surface floodplain through a manhole in a typical setup of an urban drainage system. Both models can be utilized for a complete unsteady hydrograph, ranging from inflow from the floodplain into non-surcharging sewer to overflow of the surcharging sewer. When compared to the commonly utilized weir/orifice approach to calculating exchange volumes (Nasello and Tucciarelli, 2005; Seyoum et al., 2012), the quasi-steady model explicitly accounts for the head losses along the flow path from the sewer pipe to the surface and links the exchange flow to the total head in the sewer pipe minus the occurring head losses. The dynamic model also takes into account the head losses but is also able to estimate the evolution of the water level in the manhole with the aid of one additional boundary condition at the downstream sewer pipe.

The models were calibrated with steady flow data from large-scale experiments from Rubinato et al. (2017) and were validated against unsteady flow conditions in the same experimental setup. Both models exhibited good agreement with the experimental measurements, with the dynamic model performing a little better with a Nash–Sutcliffe efficiency coefficient for the unsteady section of each tested hydrograph ranging between 0.667 and 0.982. The dynamic model captured better the physics of the problem since it was able to reproduce to a certain degree the suction in the manhole that was observed at the falling limb of the hydrograph. Both models performed significantly better than the standard weir/orifice formulations for exchange volume as evaluated in Rubinato et al. (2017). Past work suggests lumping head losses into a single coefficient, which has resulted in a wide range of calibrated discharge coefficients. These existing methods may be sensitive to the choice of boundary condition/measurement location as well as to the

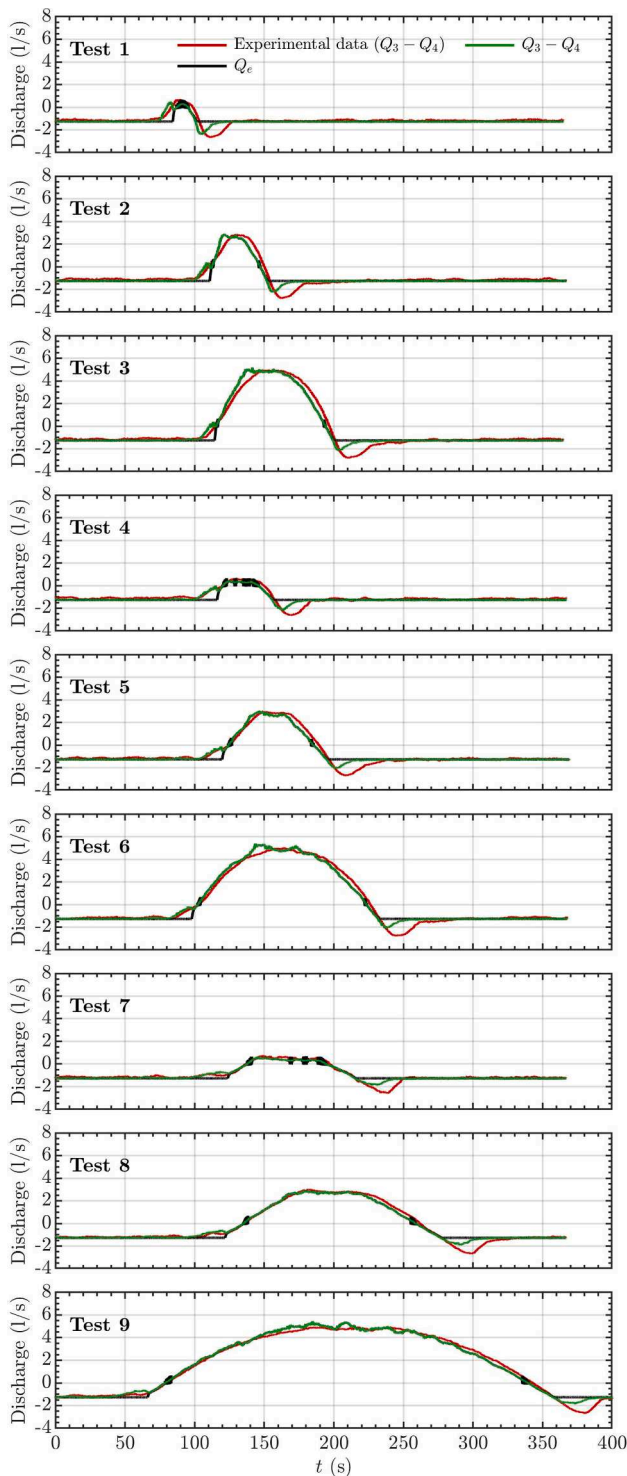


Fig. 8. Comparison of Q_e and $Q_3 - Q_4$ predicted by the dynamic model against data from the experiments of Rubinato et al. (2017).

method of calculation of pipe/surface hydraulic head (Rubinato et al., 2018a).

The utilization of the models at larger geometrical scales can be facilitated by using non-dimensional variables, such as the Froude number within the hypothetical surface and the Reynolds numbers in the pipe and in the manhole. The values of these non-dimensional variables are provided in Rubinato et al. (2017). The hydraulic conditions replicated include fully turbulent pipe flows and subcritical flow conditions in reasonably flat floodplains. A topic of further work would be

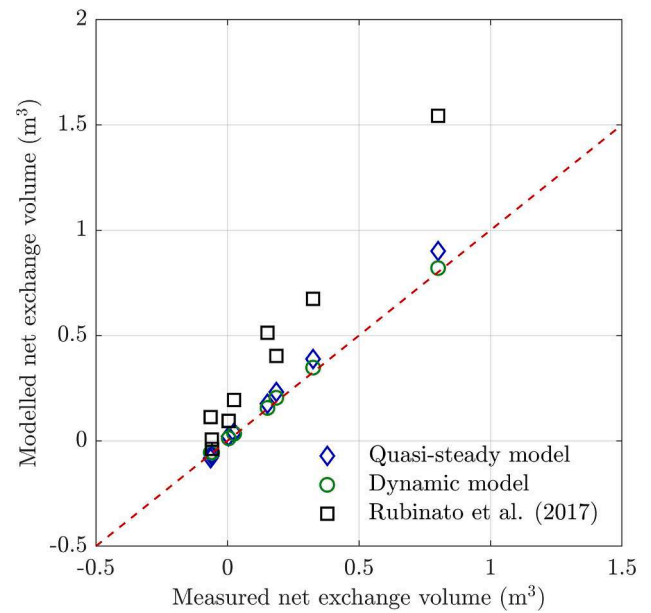


Fig. 9. Comparison of the modelled and measured net exchange volumes of water between the sewer and the floodplain for the unsteady part of each hydrograph from Fig. 7.

to consider scale effects and transferability of energy loss parameters to full size systems, as well as the transferability of the findings and parameter sensitivity to different flow conditions and geometrical configurations. Given an understanding of the relevant boundary conditions via measurements or hydrodynamic modelling, the methodology of this study could be applied to systems with multiple interaction nodes and/or with lids covering the manholes. Further experimental work could consider the calibration of energy loss parameters in such systems and sensitivity of flood modelling predictions to these parameters.

Besides the development of the two models and the demonstration of their satisfactory predictive capabilities in unsteady flow conditions, this study also suggests that the head losses that occur in the considered dual drainage system consist mostly of the head losses due to the flow expansion at the location where the sewer pipe meets the manhole. Frictional head losses in the sewer pipe are an order of magnitude smaller, while the frictional head losses in the manhole and the head losses where the flow exits the manhole at the surface are negligible, due to the significantly lower velocities involved. Therefore, in order to produce more transferable, standardized energy loss coefficients to describe flow exchange from sewer systems to surface flows, it is suggested that future work focuses on measuring sub-surface pipe/exchange structure hydraulic losses in flood/high flow conditions. It is noted that an extensive body of work already exists on head losses through such structures in non-surcharging/flooding conditions (e.g. Marsalek, 1985; Pedersen and Mark, 1990), and the feasibility of data from these studies to provide initial estimates of energy losses for use in flood conditions could be investigated.

CRedit authorship contribution statement

Vasileios Kitsikoudis: Conceptualization, Formal analysis, Investigation, Methodology, Software, Writing - original draft, Writing - review & editing. **Sebastien Erpicum:** Conceptualization, Investigation, Writing - review & editing. **Matteo Rubinato:** Conceptualization, Investigation, Data curation, Methodology, Writing - original draft, Writing - review & editing. **James D. Shucksmith:** Conceptualization, Investigation, Methodology, Writing - original draft, Writing - review & editing. **Pierre Archambeau:** Conceptualization, Data curation. **Michel Piroton:** Conceptualization. **Benjamin Dewals:** Conceptualization,

Investigation, Methodology, Supervision, Writing - original draft, Writing - review & editing.

Declaration of Competing Interest

The authors declare that they have no known competing financial interests or personal relationships that could have appeared to influence the work reported in this paper.

Appendix

The model of Idelchik (2007) considers a diverging tee and calculates the parameter k_2 with the following equation:

$$k_2 = 1 + \left(\frac{Q_c A_p}{Q_3 A_m} \right)^2 \quad (13)$$

The parameter k_2 with the model of Hager (2010) is given by:

$$k_2 = 1 - 2 \frac{Q_c}{Q_3} \cos\left(\frac{3}{4}\theta\right) + \left(\frac{Q_c}{Q_3}\right)^2 \quad (14)$$

where θ is the angle between the manhole and the sewer pipe, which herein is equal to 90° .

References

- Arrault, A., Finaud-Guyot, P., Archambeau, P., Bruwier, M., Ercicum, S., Piroton, M., Dewals, B., 2016. Hydrodynamics of long-duration urban floods: experiments and numerical modelling. *Nat. Hazards Earth Syst. Sci.* 16 (6), 1413–1429.
- Bazin, P.-H., Nakagawa, H., Kawaike, K., Paquier, A., Mignot, E., 2014. Modeling Flow Exchanges between a Street and an Underground Drainage Pipe during Urban Floods. *J. Hydraul. Eng.* 140 (10), 04014051. [https://doi.org/10.1061/\(ASCE\)HY.1943-7900.0000917](https://doi.org/10.1061/(ASCE)HY.1943-7900.0000917).
- Beg, M.N.A., Carvalho, R.F., Tait, S., Brevis, W., Rubinato, M., Schellart, A., Leandro, J., 2018. A comparative study of manhole hydraulics using stereoscopic PIV and different RANS models. *Water Sci. Technol.* 2017, 87–98.
- Beg, M.d., Rubinato, M., Carvalho, R., Shucksmith, J., 2020. CFD Modelling of the Transport of Soluble Pollutants from Sewer Networks to Surface Flows during Urban Flood Events. *Water* 12 (9), 2514. <https://doi.org/10.3390/w12092514>.
- Beven, K., 2006. A manifesto for the equifinality thesis. *J. Hydrol.* 320 (1–2), 18–36.
- Chen, A., S. Djordjević, J. Leandro, and D. Savić. 2007. The urban inundation model with bidirectional flow interaction between 2D overland surface and 1D sewer networks. Pages 465–472 Novatech.
- Djordjevic, S., D. Prodanovic, C. Maksimovic, M. Ivetic, and D. Savic. 2005. SIPSON – Simulation of Interaction between Pipe flow and Surface Overland flow in Networks. *Water Sci. Technol.* 52:275–283.
- Dong, B., Xia, J., Zhou, M., Deng, S., Ahmadian, R., Falconer, R.A., 2021. Experimental and numerical model studies on flash flood inundation processes over a typical urban street. *Adv. Water Resour.* 147, 103824. <https://doi.org/10.1016/j.advwatres.2020.103824>.
- Dottori, F., Di Baldassarre, G., Todini, E., 2013. Detailed data is welcome, but with a pinch of salt: Accuracy, precision, and uncertainty in flood inundation modeling. *Water Resour. Res.* 49 (9), 6079–6085.
- Fraga, L., Cea, L., Puertas, J., 2015. Validation of a 1D–2D dual drainage model under unsteady part-full and surcharged sewer conditions. *Urban Water J.* 14 (1), 74–84.
- Gómez, M., Russo, B., Tellez-Alvarez, J., 2019. Experimental investigation to estimate the discharge coefficient of a grate inlet under surcharge conditions. *Urban Water J.* 16 (2), 85–91.
- Graber, S.D., 2010. Manifold Flow in Pressure-Distribution Systems. *J. Pipeline Syst. Eng. Pract.* 1 (3), 120–126.
- Hager, W.H. (Ed.), 2010. *Wastewater Hydraulics*. Springer Berlin Heidelberg, Berlin, Heidelberg.
- Hare, C.M., 1983. Magnitude of Hydraulic Losses at Junctions in Piped Drainage Systems. *Institution of Engineers (Australia) Civ. Eng. Trans.* CE 2, 71–77.
- Idelchik, I. E. 2007. *Handbook of Hydraulic Resistance*. (A. S. Ginevskiy and A. V. Kolesnikov, Eds.), 4th edition. Begell House, translated by G. R. Malysavskia.
- Kemper, S., Schlenkhoff, A., 2019. Experimental study on the hydraulic capacity of grate inlets with supercritical surface flow conditions. *Water Sci. Technol.* 79, 1717–1726.
- Leandro, J., Chen, A.S., Djordjević, S., Savić, D.A., 2009. Comparison of 1D/1D and 1D/2D Coupled (Sewer/Surface) Hydraulic Models for Urban Flood Simulation. *J. Hydraul. Eng.* 135 (6), 495–504.
- Lopes, P., Leandro, J., Carvalho, R.F., Páscoa, P., Martins, R., 2015. Numerical and experimental investigation of a gully under surcharge conditions. *Urban Water J.* 12 (6), 468–476.
- Machiels, O., Ercicum, S., Archambeau, P., Dewals, B., Piroton, M., 2011. Theoretical and numerical analysis of the influence of the bottom friction formulation in free surface flow modelling. *Water SA* 37, 221–228.
- Marsalek, J. 1985. Head Losses at Selected Sewer Manholes. *American Public Works Association Special Report* 52.
- Martins, R., Kesserwani, G., Rubinato, M., Lee, S., Leandro, J., Djordjević, S., Shucksmith, J.D., 2017. Validation of 2D shock capturing flood models around a surcharging manhole. *Urban Water J.* 14 (9), 892–899.
- Martins, R., J. Leandro, and R. F. de Carvalho. 2014. Characterization of the hydraulic performance of a gully under drainage conditions. *Water Sci. Technol.* 69: 2423–2430.
- Martins, R., Rubinato, M., Kesserwani, G., Leandro, J., Djordjević, S., Shucksmith, J.D., 2018. On the Characteristics of Velocities Fields in the Vicinity of Manhole Inlet Grates During Flood Events. *Water Resour. Res.* 54 (9), 6408–6422.
- McMillan, H.K., Booker, D.J., Cattoën, C., 2016. Validation of a national hydrological model. *J. Hydrol.* 541, 800–815.
- McNown, J.S., 1954. Mechanics of Manifold Flow. *Trans. Am. Soc. Civ. Eng.* 119 (1), 1103–1118.
- Moy de Vitry, M., Dicht, S., Leitão, J.P., 2017. floodX: urban flash flood experiments monitored with conventional and alternative sensors. *Earth Syst. Sci. Data* 9 (2), 657–666.
- Moy de Vitry, M., Leitão, J.P., 2020. The potential of proxy water level measurements for calibrating urban pluvial flood models. *Water Res.* 175, 115669. <https://doi.org/10.1016/j.watres.2020.115669>.
- Nasello, C., Tucciarelli, T., 2005. Dual Multilevel Urban Drainage Model. *J. Hydraul. Eng.* 131 (9), 748–754.
- Noh, S.J., Lee, S., An, H., Kawaike, K., Nakagawa, H., 2016. Ensemble urban flood simulation in comparison with laboratory-scale experiments: Impact of interaction models for manhole, sewer pipe, and surface flow. *Adv. Water Resour.* 97, 25–37.
- Pedersen, F.B., Mark, O., 1990. Head Losses in Storm Sewer Manholes: Submerged Jet Theory. *J. Hydraul. Eng.* 116 (11), 1317–1328.
- Rubinato, M., 2015. Physical scale modelling of urban flood systems. PhD Thesis. The University of Sheffield.
- Rubinato, M., Lee, S., Martins, R., Shucksmith, J.D., 2018a. Surface to sewer flow exchange through circular inlets during urban flood conditions. *J. Hydroinf.* 20, 564–576.
- Rubinato, M., Martins, R., Kesserwani, G., Leandro, J., Djordjević, S., Shucksmith, J., 2017. Experimental calibration and validation of sewer/surface flow exchange equations in steady and unsteady flow conditions. *J. Hydrol.* 552, 421–432.
- Rubinato, M., Martins, R., Shucksmith, J.D., 2018b. Quantification of energy losses at a surcharging manhole. *Urban Water J.* 15 (3), 234–241.
- Rubinato, M., Nichols, A., Peng, Y., Zhang, J.-M., Lashford, C., Cai, Y.-P., Lin, P.-Z., Tait, S., 2019. Urban and river flooding: Comparison of flood risk management approaches in the UK and China and an assessment of future knowledge needs. *Water Sci. Eng.* 12 (4), 274–283.
- Schmitt, T., Thomas, M., Etrich, N., 2004. Analysis and modeling of flooding in urban drainage systems. *J. Hydrol.* 299 (3–4), 300–311.
- Seyoum, S.D., Vojinovic, Z., Price, R.K., Weesakul, S., 2012. Coupled 1D and Noninertia 2D Flood Inundation Model for Simulation of Urban Flooding. *J. Hydraul. Eng.* 138 (1), 23–34.
- Tscheikner-Gratl, F., P. Zeisl, C. Kinzel, J. Leimgruber, T. Ertl, W. Rauch, and M. Kleidorfer. 2016. Lost in calibration: why people still do not calibrate their models, and why they still should – a case study from urban drainage modelling. *Water Sci. Technol.* 74:2337–2348.